

1. The considered system is underactuated. All the used propellers are coplanar. This condition defines the impossibility to reach some configurations because of a coupling between translation and orientation. Just a tilted configuration could be considered, on the other hand, fully actuated. By considering rotating propellers, the thrust will rotate too, and the system derives its being completely actuated. About the request to offer a formal description of the configuration space, it is possible to consider the following one:

$$C = R^3 \times SO(3), q \in C$$

$$q = \begin{bmatrix} x \\ y \\ z \\ \vartheta \\ \varphi \\ \psi \end{bmatrix}$$

The number of Degrees of freedom is equal to six.

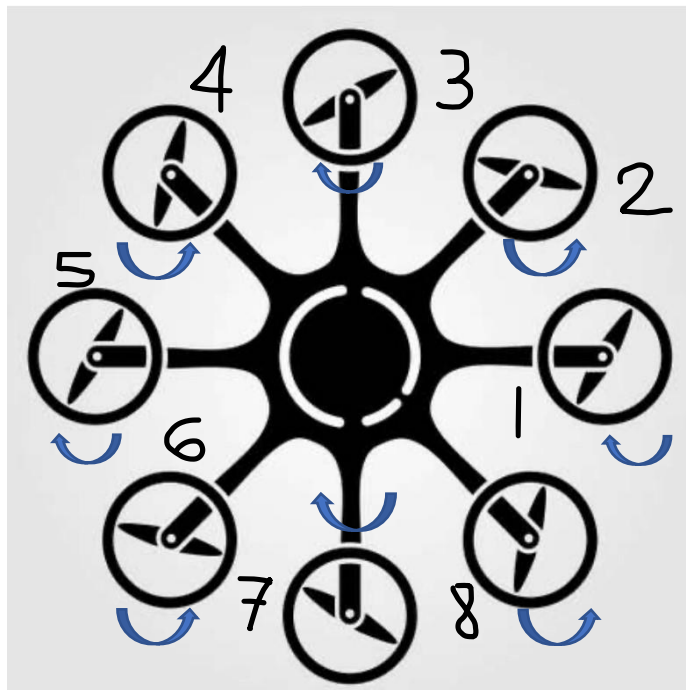


Figure 1

$$T_i = c_T \cdot \omega_i^2$$

$$Q_i = c_Q \cdot \omega_i^2$$

$$u_T = \sum_{i=1}^8 T_i$$

$$\tau_x = l \left[ (T_3 - T_7) + (T_2 - T_6) \cos\left(\frac{\pi}{4}\right) + (T_4 - T_8) \cos\left(\frac{\pi}{4}\right) \right]$$

$$\tau_y = l \left[ (T_1 - T_5) + (T_8 - T_4) \sin\left(\frac{\pi}{4}\right) + (T_2 - T_6) \sin\left(\frac{\pi}{4}\right) \right]$$

$$\tau_z = [-Q_1 + Q_2 - Q_3 + Q_4 - Q_5 + Q_6 - Q_7 + Q_8]$$

Therefore, the Allocation Matrix calculation can be completed and reported in the following form.

$$\begin{bmatrix} u_T \\ \tau_x \\ \tau_y \\ \tau_z \end{bmatrix} = \begin{bmatrix} c_T & c_T & c_T & c_T & c_T & c_T & c_T & c_T \\ 0 & \frac{\sqrt{2}}{2} l c_T & l c_T & \frac{\sqrt{2}}{2} l c_T & 0 & -\frac{\sqrt{2}}{2} l c_T & -l c_T & -\frac{\sqrt{2}}{2} l c_T \\ l c_T & \frac{\sqrt{2}}{2} l c_T & 0 & -\frac{\sqrt{2}}{2} l c_T & -l c_T & -\frac{\sqrt{2}}{2} l c_T & 0 & \frac{\sqrt{2}}{2} l c_T \\ -c_Q & c_Q & -c_Q & c_Q & -c_Q & c_Q & -c_Q & c_Q \end{bmatrix} \begin{bmatrix} \omega_1^2 \\ \omega_2^2 \\ \omega_3^2 \\ \omega_4^2 \\ \omega_5^2 \\ \omega_6^2 \\ \omega_7^2 \\ \omega_8^2 \end{bmatrix}$$

2. By considering the hierarchical control, it is possible to evaluate its hierarchical structure, which justifies its name, which allows to separate the linear part from the nonlinear one through the two-loops control architecture. The outer loop contains the linear part, and the inner loop contains the angular one. Moreover, in the inner loop, thanks to a second order filter, the noise reduction and the numerical computation of the pitch and roll time derivatives is allowed. On the other hand, this control is coordinates dependent. It motivates the presence of representative singularities which do not allow the usage of this technique to control system employed in complex flights (since the singularities in  $\vartheta = \pm\pi/2$ ).

The geometric tracking control can offer a solution to this disadvantage. It is coordinate free. It is prevented by singularities. Its goal consists of the control of those systems which evolved on nonlinear manifold, and which are not fully identified in the Euclidean space. This control is used in acrobatic flights. It is defined in  $R^3 \times SO(3)$ .

On the other hand, it just guarantees the exponential stability in condition of initial attitude error less than 90 degrees. The position error goes to zero when there is not an attitude error, and it is limited for attitude errors different to zero.

About the passivity-based control, the most important difference with respect to the others consists of the absence of a feedback linearization of the non-linear, angular part. There is not the cancellation of non-linearities, that means a higher robustness. The passivity-based control can use an estimator for the external forces and moments which act on the UAV. The estimator is based on the momentum, and it is employed to compensate the external disturbances and the unmodelled dynamics effects. The only passivity-based control, without the estimator, does not prevent the possibility to perform tracking tasks with great results. But this is true just in conditions of non-relevant unmodelled dynamics terms and unstructured environments. On the other hand, by using an estimator the control decreases in terms of declared robustness.

3. Let start to extract all the given data, through the program **data.m** developed in MATLAB. Then, by importing them in Simulink, **estimator\_def.slx**, useful matrices and functions are computed to obtain a  $r$ -order estimator architecture. In this case,  $r$  could be each value between one and four. The transfer function  $G(s)$ , involved into the gains evaluation, is then developed through the ITAE function for the poles assignment. Once fixed  $\omega_n = 1$ , it becomes possible to compute the poles and the related gains by convolution, according to the order of the estimator.
- By considering the references, in terms of disturbances

$$\tilde{f}_{e,x} = \tilde{f}_{e,y} = 1N$$

$$\tilde{\tau}_{e,z} = 0.1Nm$$

Consider the first order estimator results.

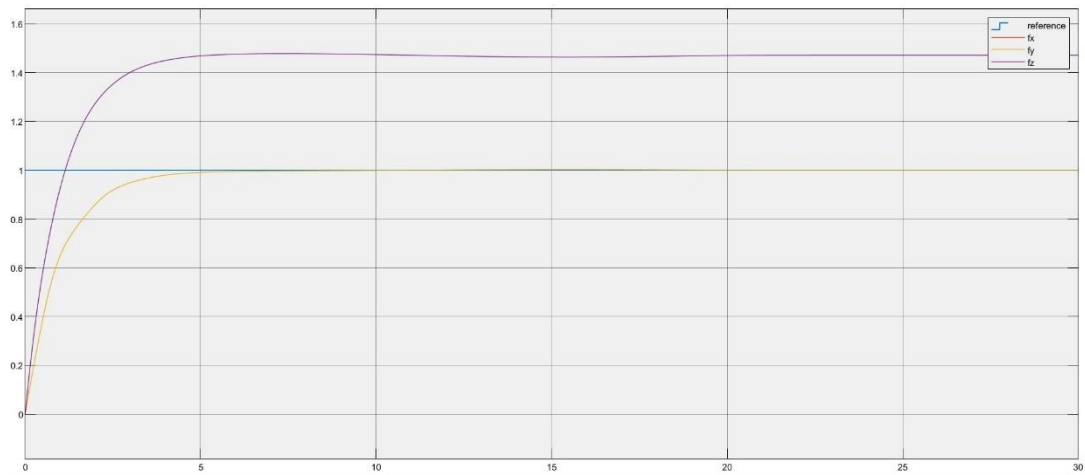


Figure 2 1st order estimator,  $f_e$  tilde

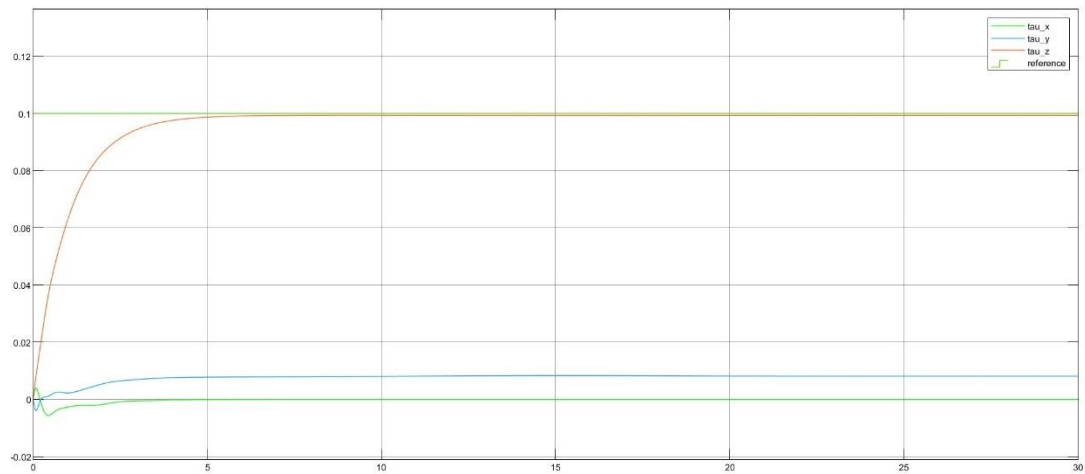


Figure 3 1st order estimator,  $\tau_e$  tilde

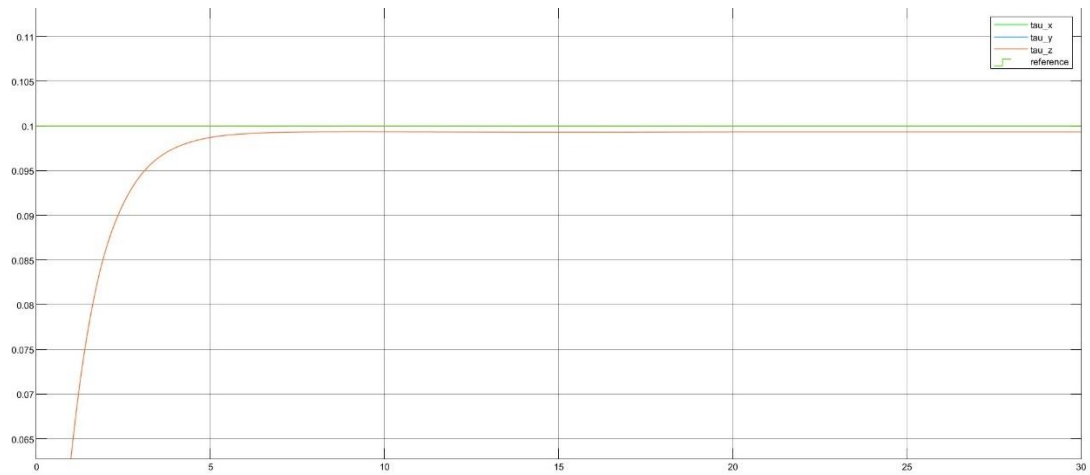


Figure 4 zoomed section of tau around z and the reference

For the first order estimator it is obtained a gain  $K1 = 1$ . In terms of disturbances along the x- and y-axis of the world frame the estimator results follow the given reference. On the other hand, in terms of estimated disturbance around the yaw axis the estimated one is close to the given reference, such as indicated in the zoomed section, but it does not reach the indicated value of  $0.1Nm$  during the simulated flight.

By increasing the estimator order, for  $r$  equal to 2 and for  $r$  equal to 3, gains are automatically calculated. Higher order estimators do not produce great differences in terms of disturbance estimations if compared with the first order one. Over elongation, depending to the poles assignment, appears and the disturbance around the yaw axis is close to the indicated reference, but it never touches that. This is proved by the following graphs.

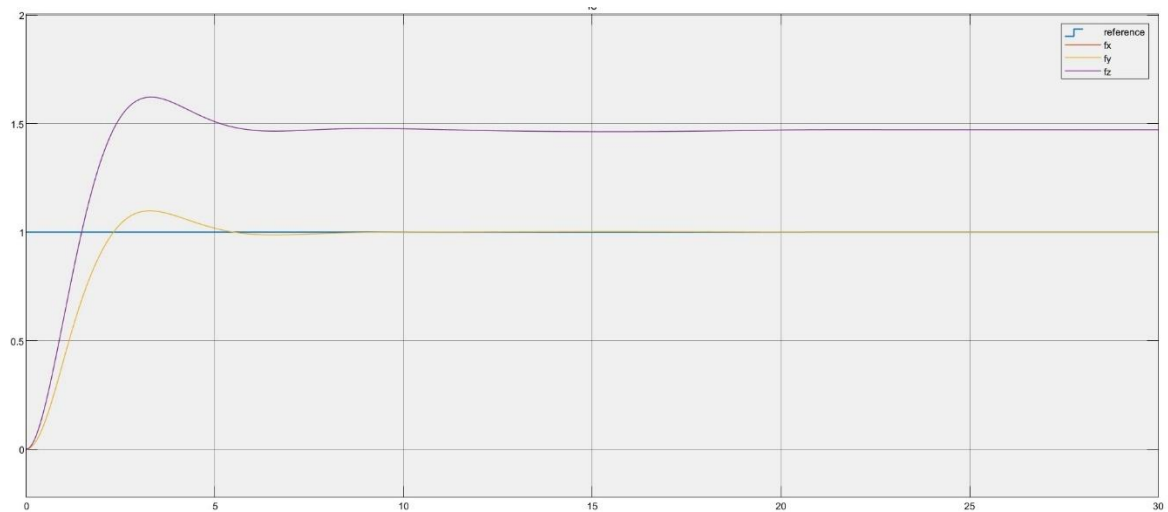


Figure 5 2nd order estimator, fe tilde

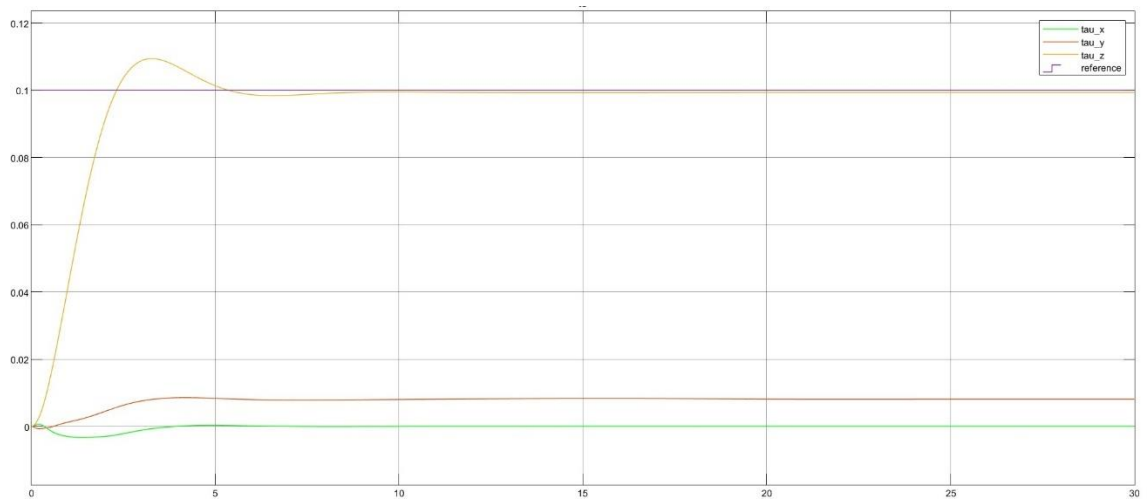


Figure 6 2nd order estimator,  $\tau$  tilde

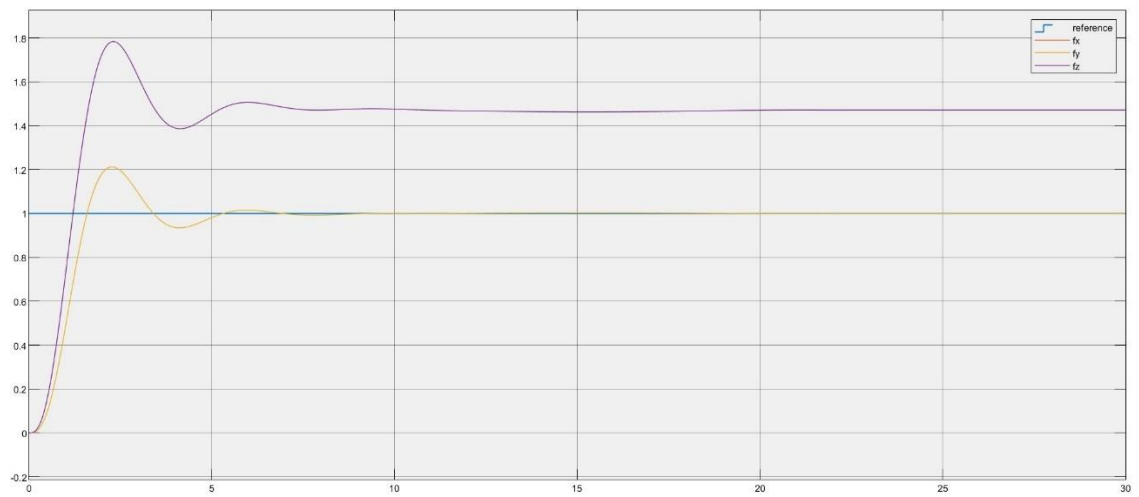


Figure 7 3rd order estimator,  $f_e$  tilde

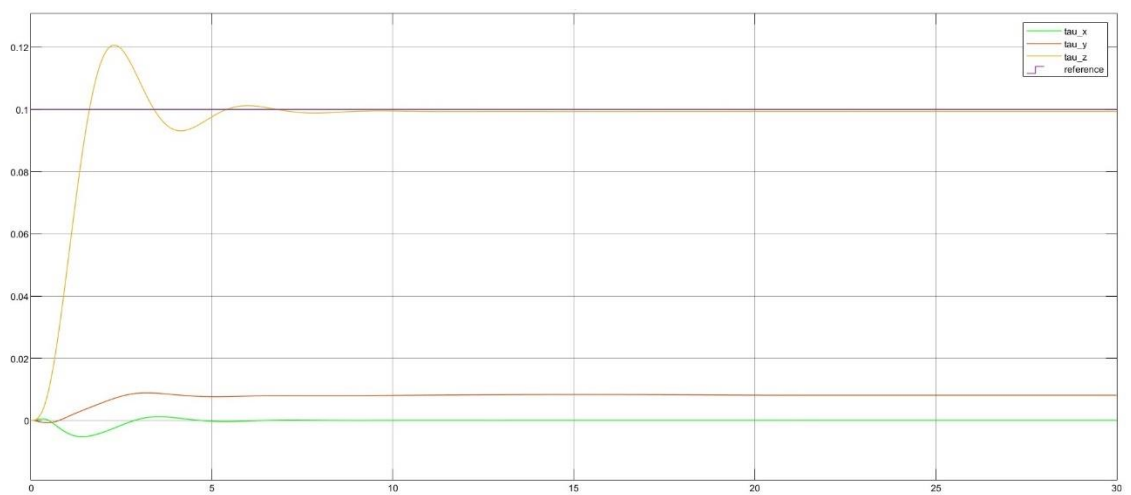


Figure 8 3rd order estimator,  $\tau$  tilde

In the second order case, the calculated gains are:

$$\begin{aligned}K1 &= 1 \\K2 &= 1.4\end{aligned}$$

And in the third order case they are equal to:

$$\begin{aligned}K1 &= 1.23 \\K2 &= 1.75 \\K3 &= 3.76\end{aligned}$$

Results degrade in terms of quality for the appearance of a previously absent over elongation. The ITAE function allows to consider, at most, a six-order estimator. But this simulation is projected to offer, at least, a fourth order estimator, as already said. In this case, the obtained gains are equal to:

$$\begin{aligned}K1 &= 0.78 \\K2 &= 1.6 \\K3 &= 2.1 \\K4 &= 19.27\end{aligned}$$

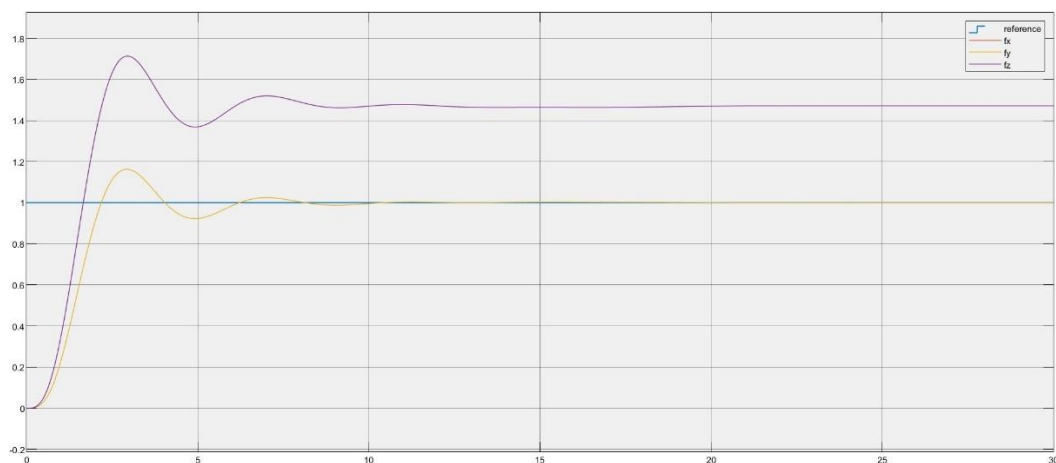


Figure 9 4th order estimator,  $f_e \tilde{t}$

By considering this result, because of an ever more relevant over elongation, the convergence to the reference is delayed.

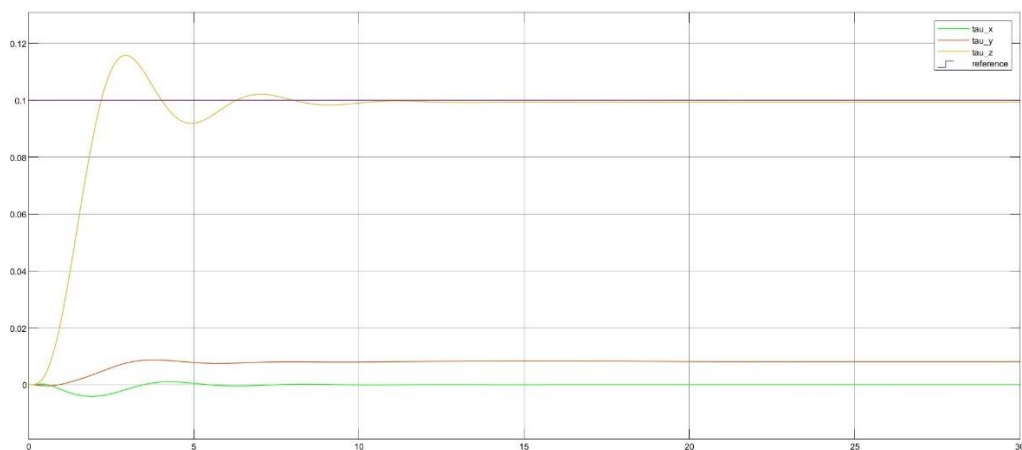


Figure 10 4th order estimator,  $\tau \tilde{t}$

In conclusion, from the second order estimator estimation results do not improve too much. It is possible to estimate the real mass of the quadrotor through the estimated disturbance along the z-axis by considering the following expression:

$$m = m_n + \hat{m} = m_n + \frac{\hat{f}_{e,z}}{g} = 1.1kg + \frac{1.478 \frac{kg \cdot m}{s^2}}{9.81 \frac{m}{s^2}} = 1.25kg$$

The disturbance effect along the z-axis could be just added to the gravity term meaning a higher real value of the mass with respect to the case in which no disturbance acts on this axis.

4. To complete the geometric control scheme, all the needed functions are calculated to project both the inner and outer loop which characterize the controller. Starting from the outer loop,  $K_p$  e  $K_v$  are respectively chosen equal to 10 and 1. The vector  $e3 = [0 \ 0 \ 1]^T$  is declared and the position and linear velocity errors are defined. At the end, the total thrust  $u_T$  and  $z_{b,des}$  are defined. Then, to build the inner loop scheme, once chosen  $K_r$  and  $K_w$  both equal to 100, after retrieved  $R_{b,d}$  and considered  $\omega_{b,d}^b$ , the tracking error for the angular motion are calculated through the expressions of  $err_R$  and  $err_W$ . In conclusion the torque  $\tau^b$  is obtained. All the obtained results are shown as follows and the UAV animation is uploaded in the homework folder.

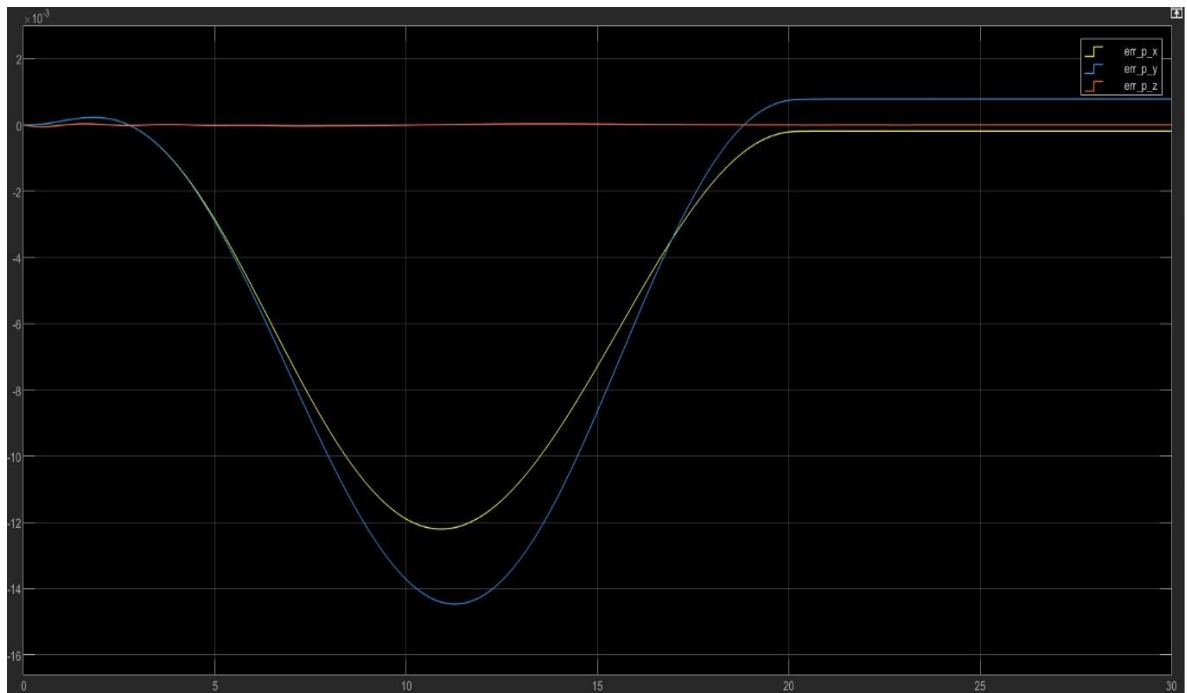


Figure 11 position error with respect to the time

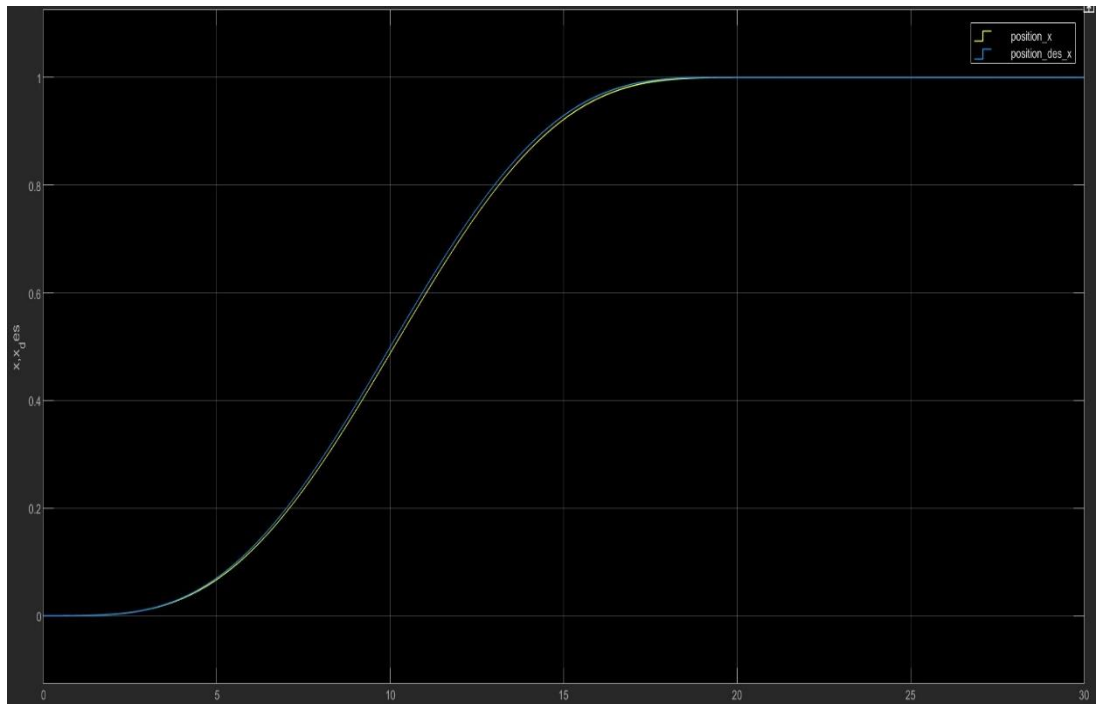


Figure 12  $x, x_{des}$  with respect to the time

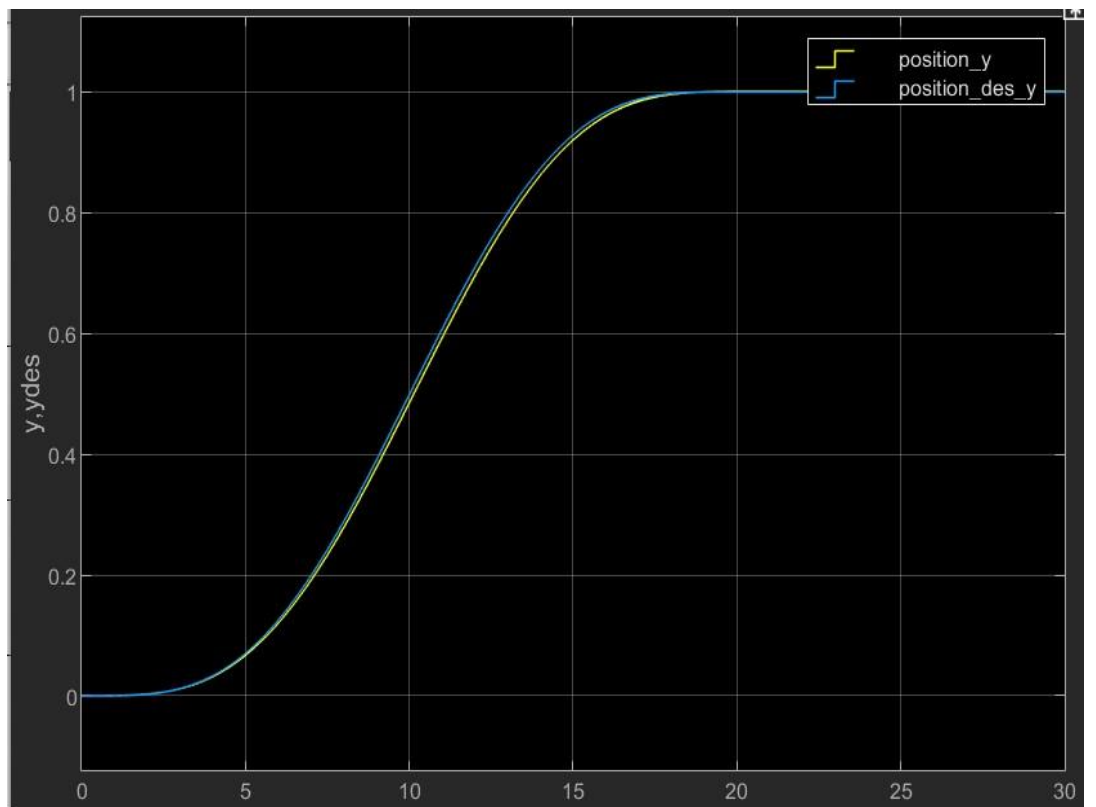


Figure 13  $y, y_{des}$  with respect to the time



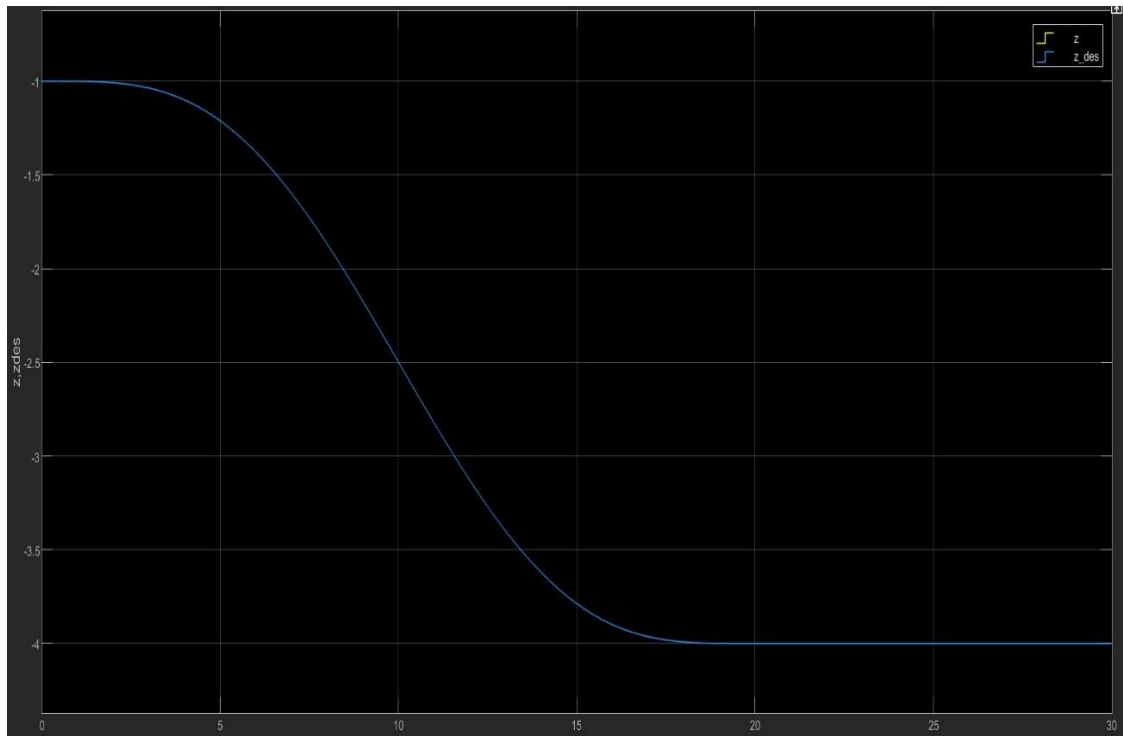


Figure 14  $z, z_{des}$  with respect to the time

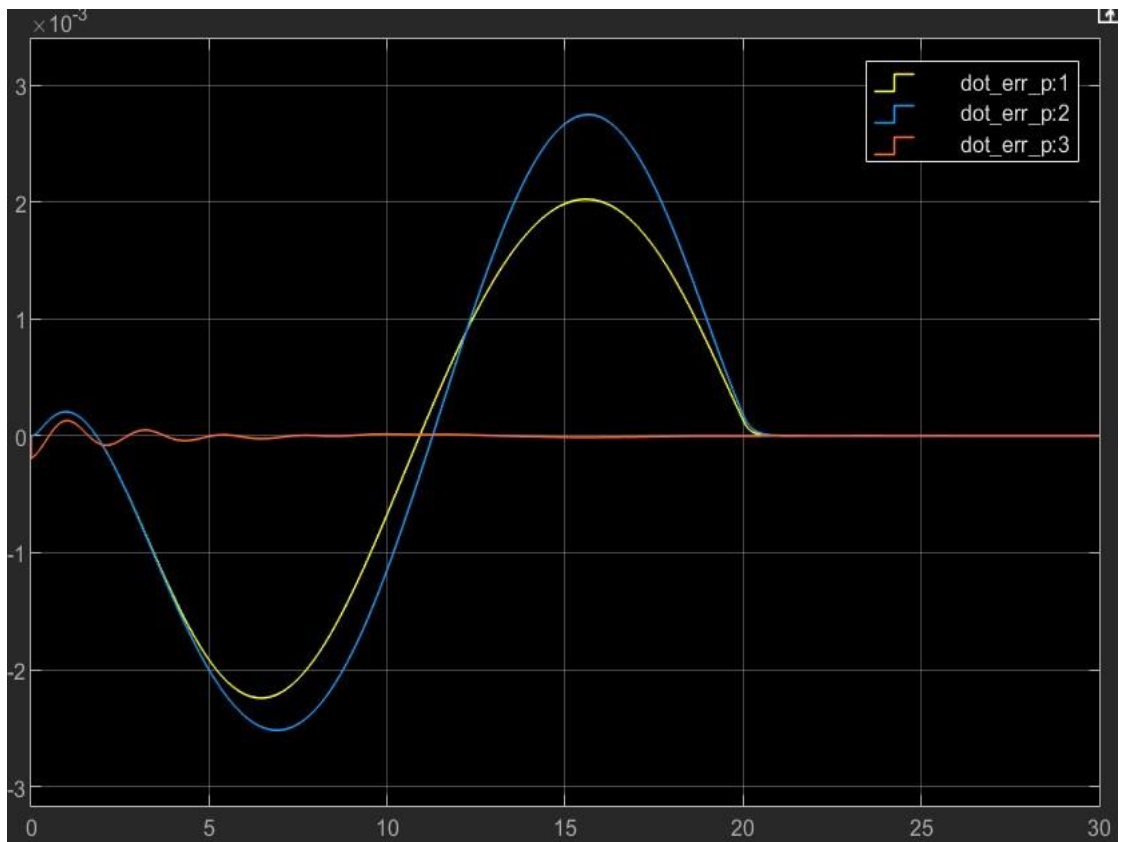


Figure 15 error linked to the linear velocity with respect to the time

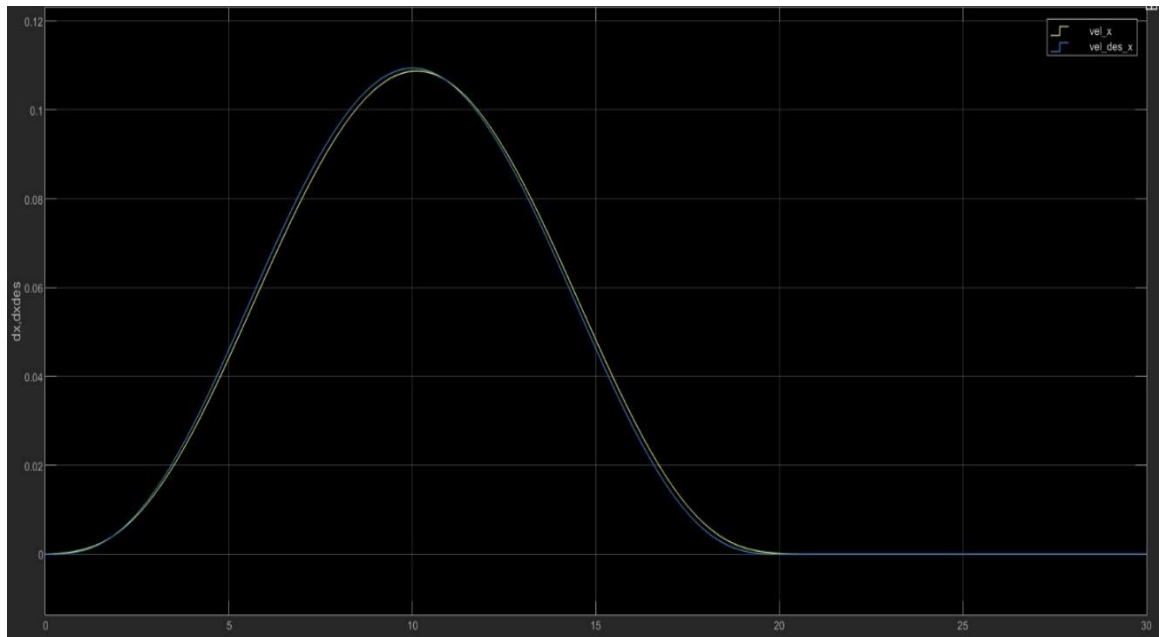


Figure 16 time derivative of  $x$  and  $x_{des}$  with respect to the time

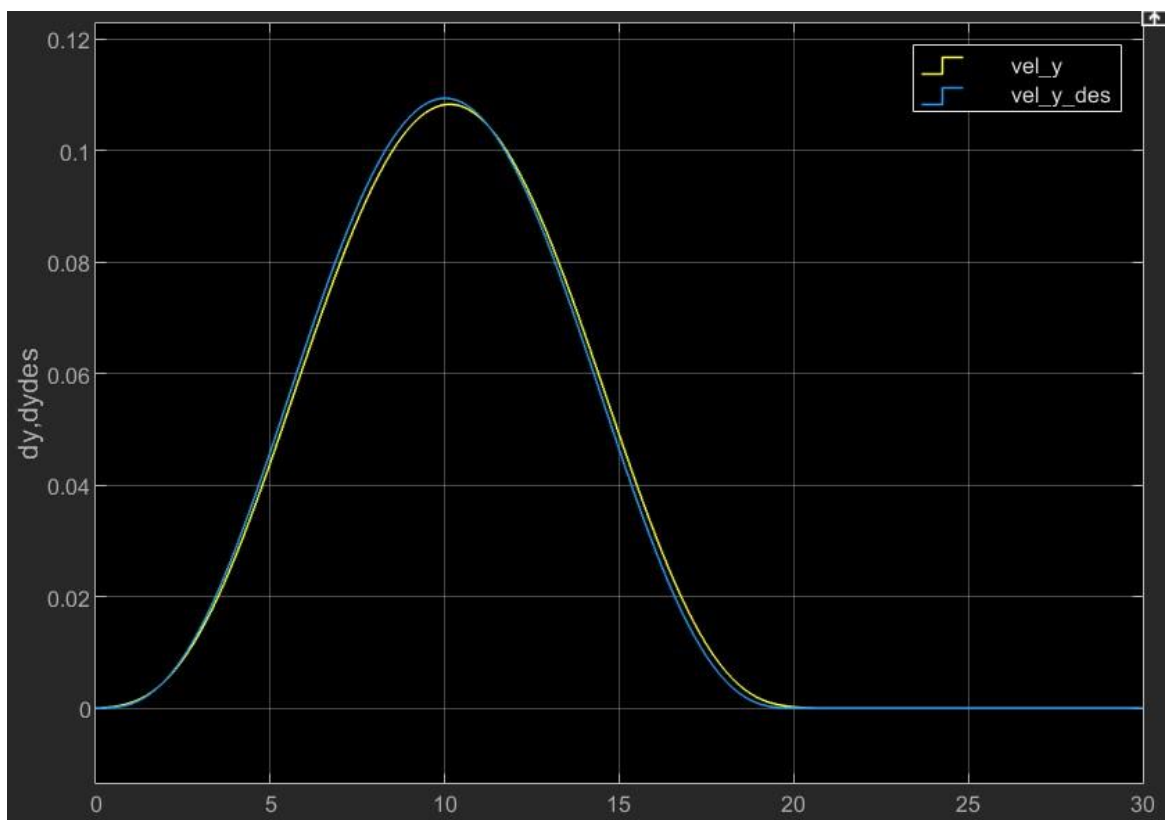


Figure 17 time derivative of  $y$  and  $y_{des}$  with respect to the time

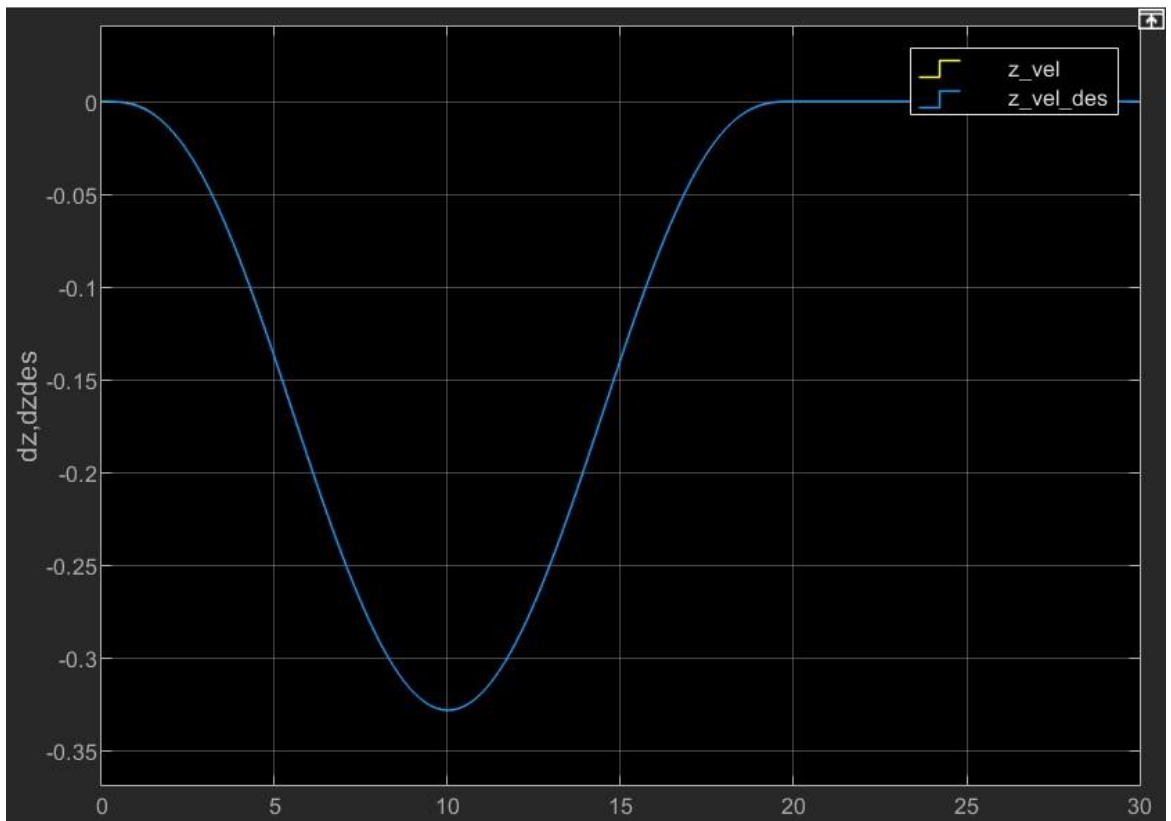


Figure 18 time derivative of  $z$  and  $z_{des}$  with respect to the time

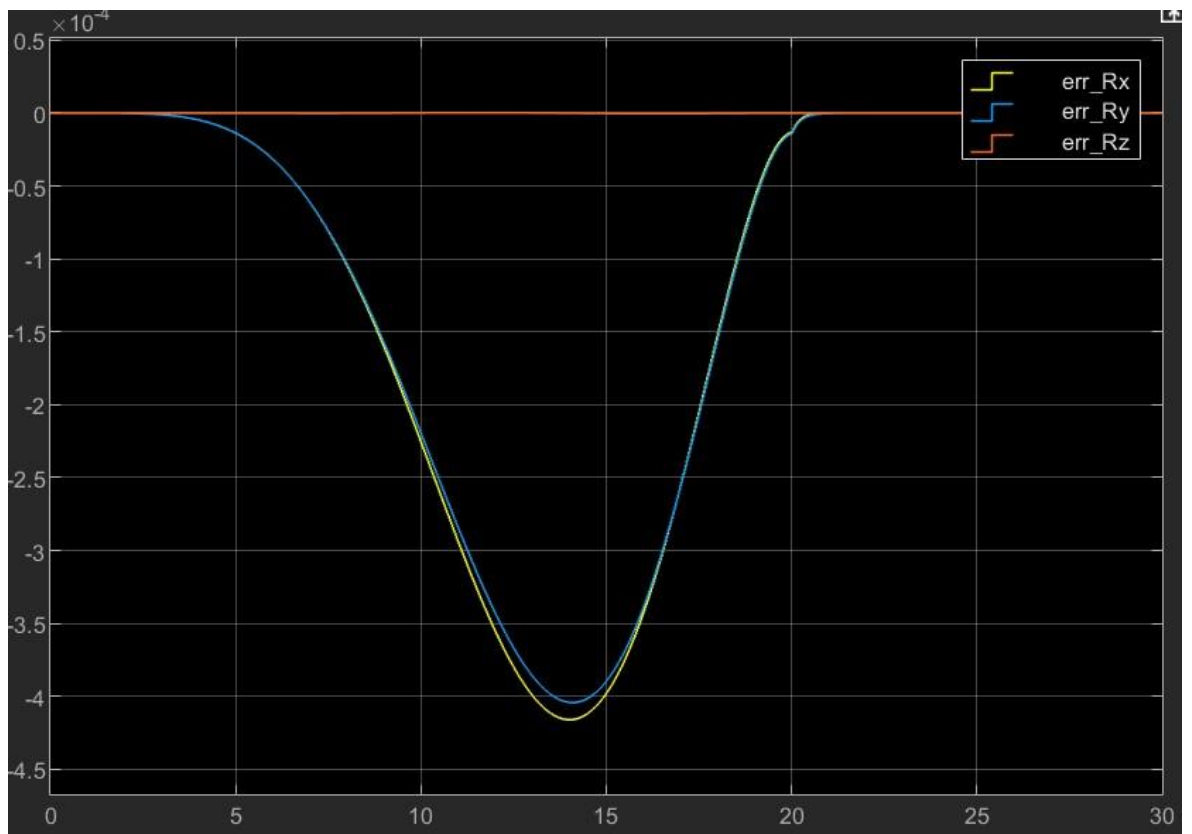


Figure 19 error  $R$  with respect to the time

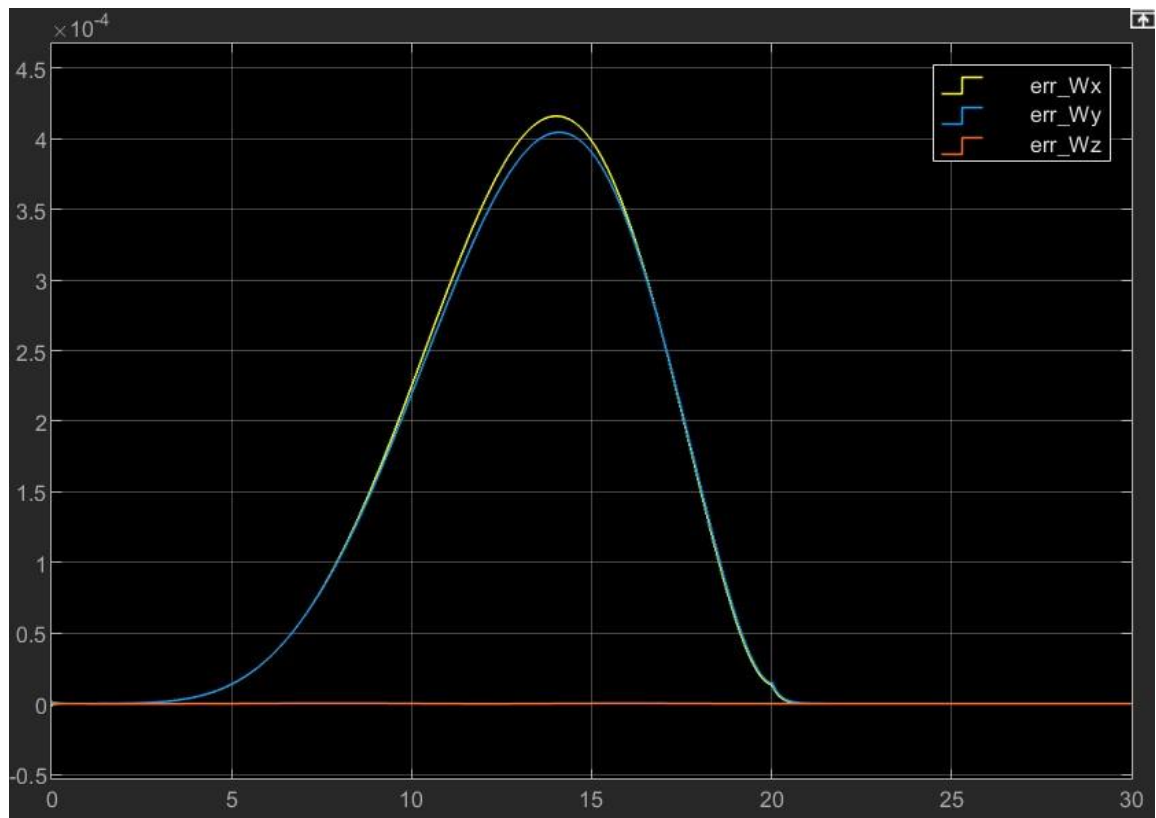


Figure 20 error\_W with respect to the time

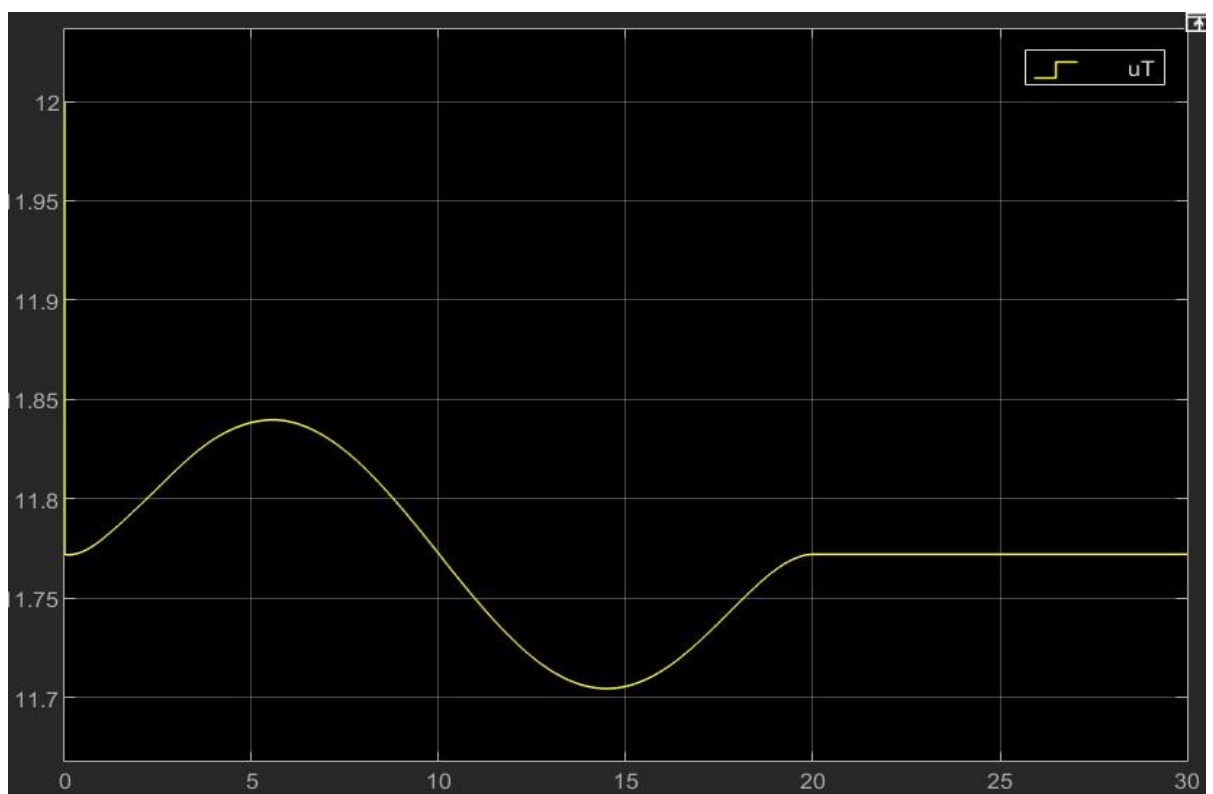


Figure 21 total thrust with respect to the time

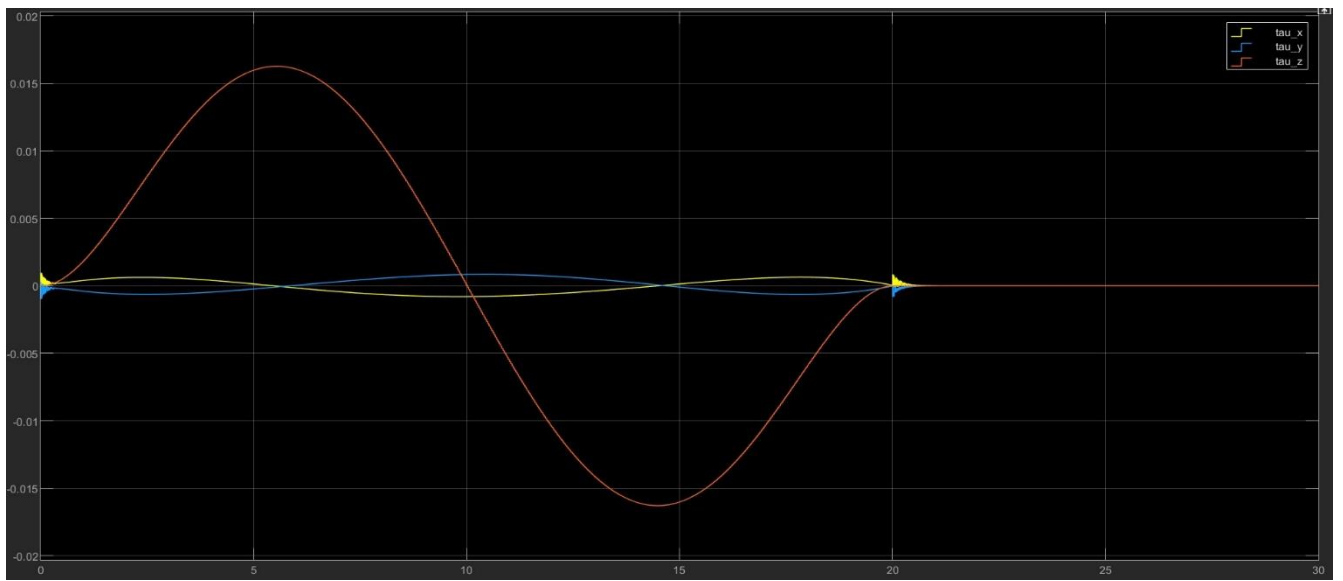


Figure 22  $\tau_b$  with respect to the time